J Solution Chem (2014) 43:585–607
DOI 10.1007/s10953-014-0146-7

Study of the Interaction Between Coenzyme Q_{10} and Human Serum Albumin: Spectroscopic Approach

Xin Peng · Yinhe Sun · Wei Qi · Rongxin Su · Zhimin He

Received: 7 September 2013 / Accepted: 20 November 2013 / Published online: 1 March 2014

Abstract UV–vis absorption, fluorescence, circular dichroism (CD) and Fourier transform infrared (FT-IR) spectroscopic methods were employed to reveal the mechanism of the binding between coenzyme Q_{10} (CoQ_{10}) and human serum albumin (HSA) under simulated physiological conditions (pH = 7.4). The binding parameters were calculated by the fluorescence quenching method. The results demonstrate that the fluorescence quenching of HSA by CoQ_{10} is mainly static quenching due to the formation of HSA–CoQ_{10} complexes, and the number of binding sites (n) is equal to 1. The thermodynamic parameters ($\Delta H^0 = -43.18$ kJ·mol^{-1}, $\Delta S^0 = -47.05$ J·mol^{-1}·K^{-1}, $\Delta G^0 = -29.15$ kJ·mol^{-1}) indicate that the enthalpy-driven binding process is favorable, and the main binding forces between CoQ_{10} and HSA are hydrogen bonds and van der Waals forces. The competitive experiments using different site markers indicate that subdomain IIA (site I) of HSA is the primary binding site for CoQ_{10}. The average binding distance (r) between HSA and CoQ_{10} is 4.29 nm, which was estimated according to the Förster's theory of non-radiation energy transfer. In addition, the UV–vis absorption, synchronous fluorescence, three-dimensional

X. Peng
School of Life Sciences, Tianjin University, Tianjin 300072, People's Republic of China

X. Peng · Y. Sun · W. Qi (✉) · R. Su · Z. He
Chemical Engineering Research Center, School of Chemical Engineering and Technology, Tianjin University, Tianjin 300072, People's Republic of China
e-mail: qiwei@tju.edu.cn

W. Qi · R. Su · Z. He
State Key Laboratory of Chemical Engineering, Tianjin University, Tianjin 300072, People's Republic of China

W. Qi · R. Su
Tianjin Key Laboratory of Membrane Science and Desalination Technology, Tianjin University, Tianjin 300072, People's Republic of China

W. Qi · R. Su · Z. He
The Co-Innovation Center of Chemistry and Chemical Engineering of Tianjin, Tianjin, People's Republic of China

fluorescence, 8-anilino-1-naphthalenesulfonic acid fluorescence, CD spectra, and FT-IR spectroscopy data show slight conformational changes of HSA in the presence of CoQ_{10}. These findings provide valuable binding information between HSA and CoQ_{10}, which may be beneficial to pharmacokinetics research and could be used to design the dosage form of CoQ_{10}.

Keywords Coenzyme Q_{10} · Human serum albumin · UV–vis absorption · Fluorescence spectroscopy · Fourier transform infrared spectra · Circular dichroism

1 Introduction

Human serum albumin (HSA) is the most prominent protein in blood plasma and serves as a protein storage component and its physiological functions are of great importance [1]. Analysis of the crystal structure has revealed that HSA is composed of a single largely α-helix polypeptide chain with 585 amino acid residues, and contains three structural domains (I–III) and numerous potential drug binding sites [2]. Although its primary function is to transport fatty acids, HSA also plays an important role in the binding, transportation and distribution of many kinds of ligands, including drugs, metabolites, amino acids, steroids and metal ions, among others [3, 4]. It is universally considered that the effectiveness of drugs depends on their binding ability to proteins. The binding affinity also affects the rate at which the drug is released to sites of catabolism or pharmacological action. Thus the interaction of drugs with proteins is very significant in pharmacology and pharmacodynamics. Moreover, there are numerous proteins in the circulatory system, but it is reported that the free fraction of drugs in plasma is mainly determined by the degree of their binding to HSA [5]. Hence, due to its clinical and pharmaceutical significance, HSA has been widely used as a model protein in evaluating protein–drug interactions [6–8].

Coenzyme Q_{10} (CoQ_{10}, ubiquinone) exists in all body cells, and acts as an electron carrier of the respiratory chain in mitochondria, so it is vital to a series of activities related to energy metabolism [9]. The CoQ_{10} molecule contains a long isoprenoid chain and its structure is shown in Fig. 1. Nowadays, various CoQ_{10} products are available on the worldwide market, and CoQ_{10} is widely consumed by humans as a food supplement since it is well known as an important nutrient in supporting health and as an inhibitor in ageing [10, 11]. CoQ_{10} is also commonly used as a therapeutic agent in cardiovascular, degenerative neurologic and neuromuscular diseases [12], because it is a powerful lipophilic antioxidant protecting lipoproteins and cell membranes [13, 14]. Research also indicates that CoQ_{10} has a good effect in inhibiting the growth of human cancer cells [15]. Because of its significant value in the field of medicine and health care, considerable research has focused on the extraction [16], synthesis [17, 18], and also the interaction of CoQ_{10} with other molecules [10].

Different spectroscopic approaches have been used to detect the binding of protein with various drugs due to their high sensitivity, rapidity, and ease of implementation [8]. For example, the binding of polyphenols to bovine serum albumin and human salivary α-amylase [19], isoflavones to HSA [20], salvianolic acid B to HSA [21], and niflumic acid to HSA [22] were all investigated. However, the interaction of CoQ_{10} with HSA is seldom explored at the molecular level, so it is of interest to investigate the binding of CoQ_{10} to HSA. Moreover, drug–protein interaction is a hot and central issue in the fields of

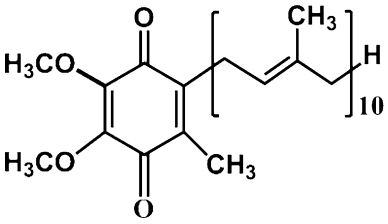

Fig. 1 Chemical structure of coenzyme Q_{10}

medicine, chemistry and biology. Increasing clinical and pharmaceutical interest in serum albumins derives from their effects on the drug of pharmacokinetics.

In this paper, the interaction mechanism between CoQ_{10} and HSA has been explored in detail for the first time by using a combination of spectroscopic methods, including UV–vis absorption, fluorescence, circular dichroism (CD) and Fourier transform infrared (FT-IR) spectra. Fluorescence quenching constants were calculated and the quenching mechanism was analyzed. The binding constants, the number of binding sites, the distance of binding and thermodynamic parameters were also obtained to illustrate the mechanism of binding. The primary binding site for CoQ_{10} on HSA was confirmed by competitive experiments using three different site markers. Moreover, the binding effect of CoQ_{10} on the conformation of HSA was investigated. These results can give us a better understanding of this biological action in vivo and may provide useful information for pharmacology and clinical research.

2 Experimental

2.1 Materials

HSA (≥98 %), ibuprofen and 8-anilino-1-naphthalenesulfonic acid (ANS) were obtained from Sigma-Aldrich (Shanghai, China) and used without further purification. CoQ_{10} (≥98.5 %, analytical standard), warfarin and digitoxin were purchased from Aladdin Reagent Co., Ltd. (Shanghai, China). The stock solutions of HSA (1.0×10^{-5} mol·L^{-1}) were prepared in 0.02 mol·L^{-1} phosphate buffer of pH = 7.40 with 0.10 mol·L^{-1} NaCl and were kept in the dark at 4 °C. HSA solutions were prepared based on their molecular weight of 66,478 g·mol^{-1}. CoQ_{10} was first dissolved in absolute ethanol (HPLC grade) with a concentration of 1.0×10^{-3} mol·L^{-1} under ultrasonic assistance, and then diluted with the phosphate buffer to obtain the CoQ_{10} solutions. ANS was prepared in 3.0×10^{-3} mol·L^{-1} stock solutions by dissolving an appropriate amount of the compound in absolute ethanol. All the other chemicals were of analytical reagent grade and double-distilled water was used throughout the experiments. The above phosphate buffer solution was used as the blank for all the samples in this study. All solutions were degassed in an ultrasonic bath prior to use.

2.2 Methods

2.2.1 UV–Vis Absorption Spectroscopy

The UV–vis spectra were measured in the range of 200–500 nm at room temperature on a TU-1810SPC spectrophotometer (Puxi General Instrument Ltd. of Beijing, China) equipped with 1.0 cm quartz cells and UVwin5.0 analysis software. The UV–vis absorption spectra of CoQ_{10}, HSA and the CoQ_{10}–HSA system (molar ratio 1:1) were measured.

2.2.2 Fluorescence Spectroscopy

All fluorescence spectra were measured on a FluoroLog 3 spectrofluorimeter (Horiba Jobin Yvon Scientific, America) equipped with 1.0 cm quartz cells and a thermostatic bath. The widths of both the excitation slit and the emission slit were set at 2.0 nm for all of the measurements. 280 nm was chosen as excitation wavelength, and the emission spectra were recorded from 290 to 500 nm. A 3.0 mL solution of 5.0×10^{-6} mol·L^{-1} HSA was titrated with CoQ_{10} (0–3.0×10^{-5} mol·L^{-1}) at three different temperatures (298, 308 and 310 K). Titrations were done manually by using a micro-injector. All solutions were mixed thoroughly and kept 10 min before measurements.

The competitive experiments were performed at 298 K using three different site markers, warfarin for site I, ibuprofen for site II, and digitoxin for site III. The concentrations of HSA and the markers were fixed at 5.0×10^{-6} mol·L^{-1}. HSA and the corresponding marker solution were first mixed together and then allowed to stand and then gradually titrated with CoQ_{10} solution. The fluorescence spectra were recorded in the range of 290–500 nm with excitation at 280 nm.

The synchronous fluorescence spectroscopy was carried out to investigate the conformational changes of the protein at 298 K, while the wavelength interval between excitation and emission wavelengths ($\Delta\lambda$) was fixed at 15 and 60 nm, and the fluorescence spectra were recorded from 260 to 320 nm.

Three-dimensional fluorescence spectra of HSA (5.0×10^{-6} mol·L^{-1}) and the CoQ_{10}–HSA system (molar ratio 2:1) were measured under the following conditions: the initial excitation wavelength was fixed at 200 nm with an increment of 10 nm; the number of scanning curves was 17; the emission wavelength was recorded between 230 and 550 nm; the other scanning parameters were the same as those for the fluorescence spectra of HSA.

HSA (5.0×10^{-6} mol·L^{-1}) was incubated at 277 K overnight in the absence or presence of CoQ_{10} (5.0–30.0×10^{-6} mol·L^{-1}), then ANS (15.0×10^{-6} mol·L^{-1}) was added and reacted for 10 min at 310 K in a thermostat bath. Binding of ANS–HSA was studied at 298 K using excitation at 370 nm and measuring the emission fluorescence spectra between 400 and 600 nm.

2.2.3 FT-IR Spectroscopic Measurements

The IR spectra of the protein solutions were measured at room temperature on a Bruker Vertex 70 FT-IR spectrometer (Bruker, Ettlingen, Germany) using the attenuated total reflection method with a nominal resolution of 4 cm^{-1} and 60 scans. The concentrations for HSA and CoQ_{10} for the FT-IR spectra analysis are 1.0×10^{-4} and 4.0×10^{-4} mol·L^{-1}, respectively. For the FT-IR spectra of HSA (in the free form), the absorbance of the buffer solution was firstly obtained, and then digitally subtracted from that of the protein solution to get the spectrum of the protein alone. For the HSA–CoQ_{10} system in buffer solutions (in the bound form), the same procedure was used, except that a CoQ_{10} buffer solution with the same concentration as in HSA–CoQ_{10} solution was used as the background medium.

2.2.4 CD Spectroscopic Measurements

The alterations to the secondary structure of HSA in the presence of CoQ_{10} were studied using a J-810 CD spectrometer (JASCO, Japan) at room temperature, using a quartz cell with a path length of 2 mm in a nitrogen atmosphere, with the slit width was set at 1 nm.

Each spectrum represented the average of three separate scans with a scan speed of 100 nm·min^{-1} when the response time was set to 1 s. The ellipticity of the CD spectra was expressed in milli-degrees. For the far-UV CD experiment, the concentration of HSA was 2.5×10^{-6} mol·L^{-1}, and the detection wavelength was situated between 200 and 260 nm. The concentrations of CoQ_{10} are 0, 5.0×10^{-6}, 1.0×10^{-5} and 1.5×10^{-5} mol·L^{-1}. The spectra of the appropriate buffer solutions, run under the same conditions, were taken as the blank and subtracted from sample spectra.

3 Results and Discussion

3.1 UV–Vis Absorption Spectra

UV–vis absorption measurements were taken to explore the structural changes of the protein and to investigate protein–ligand complex formation. The absorption spectra of HSA without and with CoQ_{10} are shown in Fig. 2. It can be seen that HSA has two main absorption peaks. The strong absorption peak at about 210 nm corresponds to absorption of the protein backbone. The weak absorption peak at about 280 nm appears to be due to the aromatic amino acids [23]. With addition of CoQ_{10} –HSA solution, the intensities of the peaks at 210 and 280 nm decrease to some extent at the same time, indicating that the interaction between HSA and CoQ_{10} leads to the structural alterations of HSA. In addition, the obvious change of absorbance intensities also indicates formation of a new complex between HSA and CoQ_{10}.

3.2 The Mechanism of Fluorescence Quenching

Fluorescence is the photon emission process caused by the return of an electron from a higher energy orbital to a lower orbital; many kinds of molecular interactions can induce fluorescence quenching, such as excited-state reactions, molecular rearrangements, energy transfer, ground state complex formation and collisional quenching [24]. Fluorescence spectroscopy is widely used in the study of physico-chemical properties of proteins, protein–ligand interactions and protein dynamics. This is because almost all proteins contain naturally fluorescent amino acid residues such as tyrosine (Tyr) and tryptophan (Trp). Fluorescence spectroscopy is one of the traditional methods to investigate the properties of proteins such as stability, hydrodynamics, kinetics or ligand binding because of its exquisite sensitivity.

When using fluorescence to study a binding reaction, a requirement is that the signal should be linearly related to the concentration of species. A nonlinear dependence of the fluorescence intensity on concentration will most likely be due to the self-aggregation of species. Even more important, nonlinearity can also be caused by absorptive screening (inner filter) effects. For the protein–drug system, the inner filter effect is caused by the absorption of excitation and emission radiation of drug and protein in fluorescence experiments, which changes the intensity of fluorescence spectra of the protein, affecting the binding parameters calculated from the fluorescence analysis [23, 25]. To avoid inner filter effects, the absorbances of all samples should be less than 0.1 at the wavelength of excitation. In this paper, we calculated the sum of absorbance at the excitation wavelength (280 nm) and emission wavelength (fluorescence peak at about 340 nm) under different conditions to eliminate the inner filter effects. The fluorescence intensity can be corrected using the following relationship:

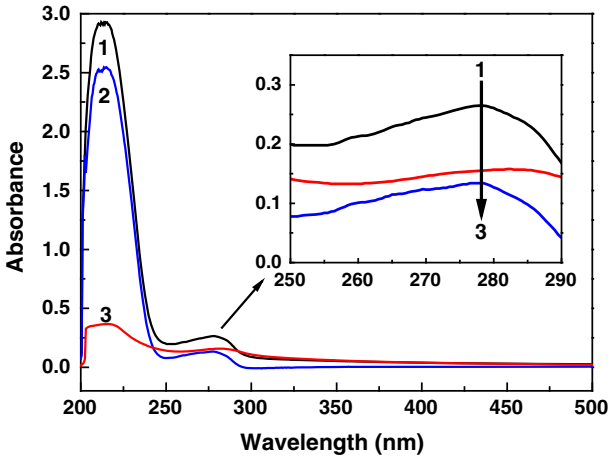

Fig. 2 UV–vis absorption spectra of HSA in the presence of CoQ_{10}. (*1*) The absorption spectrum of HSA only, (*2*) the difference absorption spectrum between CoQ_{10}–HSA and CoQ_{10} at the same concentration, and (*3*) the absorption spectrum of CoQ_{10} only. The concentrations of both HSA and CoQ_{10} were fixed at 5.0×10^{-6} mol·L^{-1}

$$F_{\text{corr}} = F_{\text{obs}} e^{(A_{\text{ex}}+A_{\text{em}})/2}, \quad (1)$$

where F_{corr} and F_{obs} are the fluorescence intensities corrected and observed, respectively, and A_{ex} and A_{em} are the absorption of the system at the excitation and emission wavelengths, respectively. The fluorescence intensity utilized in this study are the corrected data.

In order to identify the participation of Tyr and Trp groups in the interaction process between CoQ_{10} and HSA, the fluorescence of HSA excited at different wavelengths was measured in the presence of CoQ_{10}. Previous research indicated that the Tyr and Trp residues in serum albumin are excited at 280 nm; while at an excitation wavelength of 295 nm, only the Trp residue emitted fluorescence [24]. The plots of F/F_0 against [CoQ_{10}]/[HSA] are presented in Fig. 3a, where F_0 and F are the fluorescence intensities before and after the addition of CoQ_{10}, respectively. There is an obvious difference in the quenching of HSA fluorescence between two excitation wavelengths 280 and 295 nm. This indicates that both Tyr and Trp residues participate in the molecular interaction between CoQ_{10} and HSA [24].

The results of fluorescence quenching of HSA in the presence of CoQ_{10} at 298 K in the range of 290–500 nm upon excitation at 280 nm are shown in Fig. 3b. The fluorescence intensity at peak 340 nm decreased as the CoQ_{10} concentration was increased from 0 to 3×10^{-5} mol·L^{-1}, but there is no obvious change of the maximum emission wavelength or the shape of the peaks, demonstrating that the addition of CoQ_{10} led to a significant quenching of intrinsic fluorescence in HSA and that it interacts with HSA. No spectral shifts were observed for the emission spectra upon HSA–CoQ_{10} complexation, indicating that the Trp residues are not exposed to any change in polarity.

The different mechanisms of fluorescence quenching are usually divided into dynamic quenching, resulting from collisional encounters and static quenching, because of the formation of a ground-state complex between the fluorophore and quencher. These two kinds of fluorescence quenching can be distinguished by their different dependences on temperature and viscosity. For dynamic quenching, the quenching constant increases with temperature. In contrast, for static quenching, the quenching constant declines with the temperature [23]. To clarify the quenching mechanism in present case, we used the Stern–Volmer equation (Eq. 2) to analyze the fluorescence quenching data [24]:

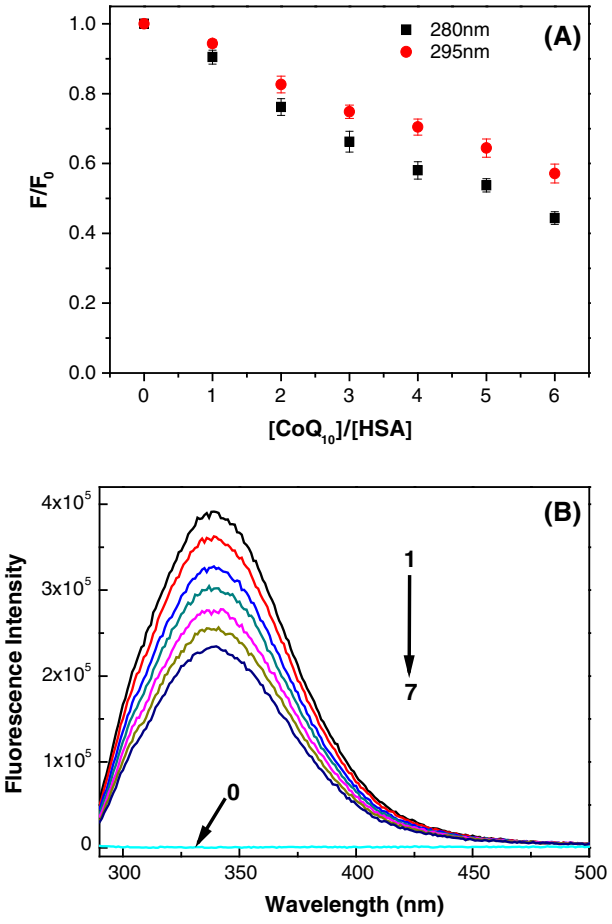

Fig. 3 **a** Fluorescence titration curves of HSA in the presence of CoQ_{10} at $\lambda_{ex} = 280$ and 295 nm; **b** fluorescence quenching spectra of HSA by CoQ_{10}, 298 K, $\lambda_{ex} = 280$ nm. The concentration of HSA was fixed at 5.0×10^{-6} mol·L^{-1}, and the concentrations of CoQ_{10} (*1–7*) are 0, 0.5, 1.0, 1.5, 2.0, 2.5 and 3.0×10^{-5} mol·L^{-1}, respectively. Curve 0 represents the fluorescence emission spectrum of CoQ_{10} only

$$\frac{F_0}{F} = 1 + k_q \tau_0 [Q] = 1 + K_{SV}[Q], \tag{2}$$

where F_0 denotes the steady-state fluorescence intensity of HSA, F is the steady-state fluorescence intensity of HSA in the presence of CoQ_{10} with various concentrations, K_{SV} is the Stern–Volmer quenching constant for the protein, [Q] is the concentration of quencher, k_q is the quenching rate constant of the biological macromolecule, and τ_0 stands for the fluorescence lifetime in the absence of quencher and it is 10^{-8} s for biomacromolecules. The plots of the Stern–Volmer equation at 298, 308 and 310 K are shown in Fig. 4a. The values of K_{SV} and k_q at 298, 308, 310 K are presented in Table 1.

In order to prove a complex formation process, the modified Stern–Volmer equation (Eq. 3) was also used for the present system [21, 26, 27]:

$$\frac{F_0}{F_0 - F} = \frac{1}{f_a K_a [Q]} + \frac{1}{f_a}, \tag{3}$$

where f_a is the fraction of accessible fluorescence, and K_a is the effective quenching constant for the accessible fluorophores. According to Eq. 3, the plots of $F_0/(F_0 - F)$ versus $[Q]^{-1}$

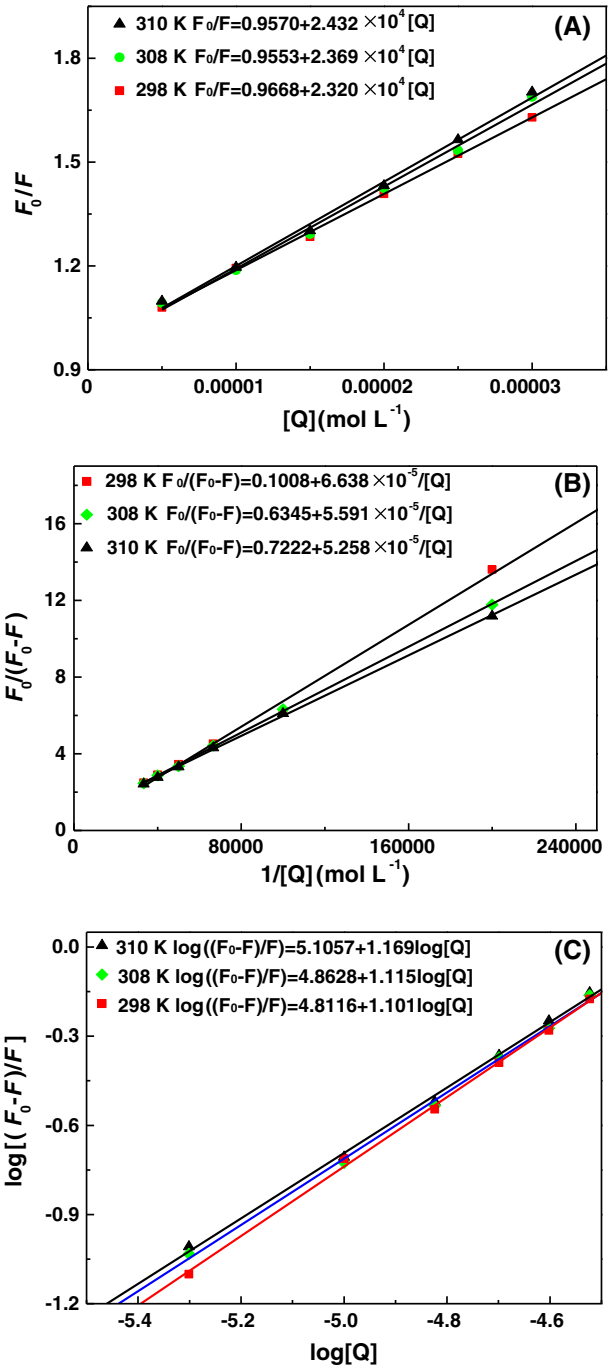

Fig. 4 **a** Stern–Volmer plots for the fluorescence quenching of HSA by CoQ_{10} at 298 (*red squares*), 308 (*green diamonds*), and 310 K (*black triangles*). **b** Modified Stern–Volmer plots for the binding of CoQ_{10} to HSA at 298 (*red squares*), 308 (*green diamonds*), and 310 K (*black triangles*). **c** Plots for calculating the number of binding sites in the HSA–CoQ_{10} system at 298 (*red squares*), 308 (*green diamonds*), and 310 K (*black triangles*) (Color figure online)

Table 1 Stern–Volmer quenching constants and modified Stern–Volmer quenching constants for the interaction of CoQ_{10} with HSA

T (K)	K_{SV} (10^4 L·mol^{-1})	k_q (10^{12} L·mol^{-1})	R	K_a (10^4 L·mol^{-1})	R
298	2.320	2.320	0.9947	0.152	0.9935
308	2.369	2.369	0.9927	1.135	0.9995
310	2.432	2.432	0.9944	1.373	0.9993

R correlation coefficient

Table 2 Binding parameters of CoQ_{10} to HSA

T (K)	K_b (10^5 L·mol^{-1})	n	R
298	1.276	1.17	0.9976
308	0.729	1.11	0.9972
310	0.648	1.10	0.9971

R correlation coefficient

are shown in Fig. 4b. The values of K_a at three temperatures are listed in Table 1. The results show that both K_{SV} and K_a increase with temperature, which suggests that the fluorescence quenching might be dynamic [21]. Since higher temperature can cause larger diffusion coefficients, the bimolecular quenching constants are expected to rise with increasing temperature. But when attention is paid to the values of k_q, we find something peculiar. Generally, the maximum scatter collision quenching constant (k_q) of various kinds of quenchers to biopolymer is 2.0×10^{-10} mol·L^{-1}·s^{-1} [26], but the values of k_q obtained in this work (Table 1) are much higher than 2.0×10^{-10} mol·L^{-1}·s^{-1}. This indicates that the quenching process is static. Additionally, we found that there are distinct changes between "the absorption spectra of HSA (Fig. 2, curve 1)" and "the difference absorption spectra between HSA–CoQ_{10} and CoQ_{10} at the same concentration (Fig. 2, curve 2)" within experimental error. This phenomenon confirms that the quenching was initiated by static quenching, because dynamic quenching only influences the excited state of quenching molecule while it has no effect on the absorption spectrum of quenching substances [27]. This phenomenon is the same as for the interaction of pyridoxine hydrochloride and diprophylline with proteins [28, 29].

3.3 Binding Constant and the Number of Binding Sites of HSA–CoQ_{10} System

For static quenching processes, when ligand molecules bind independently to a set of equivalent sites on a macromolecule, the binding constant (K_b) and the number of binding sites (n) may be calculated by using Eq. 4 [25]:

$$\log_{10}\left[\frac{F_0 - F}{F}\right] = \log_{10} K_b + n \log_{10}[Q], \tag{4}$$

where F_0, F, [Q] are the same as before. The plots of $\log_{10}$ [$(F_0 - F)/F$] versus $\log_{10}$ [Q] are shown in Fig. 4c. The values of n and K_b at 298, 308, 310 K are listed in Table 2. It can be seen that the values of n at each temperature are all close to 1, which suggests that about one molecule of CoQ_{10} is bound to one molecule of HSA. The values of K_b decrease

with increasing temperature, indicating that the binding between CoQ_{10} and HSA is affected by temperature.

3.4 Thermodynamic Parameter Analysis

Generally, there are essentially four types of non-covalent interactions that could play a leading role in ligand binding to proteins: hydrogen bonds, van der Waals forces, and hydrophobic and electrostatic interactions [30]. These can be distinguished by calculating the thermodynamic parameters, i.e. standard enthalpy (ΔH^0), standard entropy (ΔS^0) and Gibbs energy (ΔG^0). Positive values of both ΔH^0 and ΔS^0 indicate hydrophobic interactions; negative values of both ΔH^0 and ΔS^0 indicate hydrogen bond formation or van der Waals forces and, if the value of ΔH^0 is close to with a positive value of ΔS^0, this suggests an electrostatic force [21]. If ΔH^0 and ΔS^0 can be considered as constant when the temperature changes is only over a small range, then the thermodynamic parameters can be calculated by the following van't Hoff analysis using Eqs. 5 and 6:

$$\log_{10} K_b = \frac{-\Delta H^0}{2.303RT} + \frac{\Delta S^0}{2.303R}, \tag{5}$$

$$\Delta G^0 = \Delta H^0 - T\Delta S^0, \tag{6}$$

where K_b is the binding constant and R is the universal gas constant. The plot of $\log_{10} K_b$ versus T^{-1} is shown in Fig. 5a, and the values of thermodynamic parameters at 298, 308, and 310 K are presented in Table 3. The negative values of ΔG^0 at each temperature mean the binding process was spontaneous. Both ΔH^0 and ΔS^0 are negative, which indicates that van der Waals force and hydrogen-bonding are the main binding forces for the HSA–CoQ_{10} system in low dielectric solution. As shown in Fig. 5b, the change in enthalpy is the major contribution to ΔG^0, so we could say the binding is an enthalpy-driven process. In addition, from Table 2, K_b decreases with increasing temperature because the enthalpy is negative (i.e. the binding process is exothermic).

3.5 Identification of the Binding Sites of CoQ_{10} on HSA

Crystallographic analysis reveals that HSA has three structurally homologous domains (I–III), and each domain is composed of two subdomains (A and B) [31]. In order to substantiate drug binding site on HSA, competitive binding between the drug and other ligands that specifically bind to a known site or domain was scrutinized. The exceptional capability of HSA to bind various substances is predominantly dependent on the existence of two primary binding regions, namely Sudlow's sites I and II, which are located in specialized pockets in subdomains IIA and IIIA [32], respectively. Sudlow et al. [32] have proposed that site I of serum albumin shows affinities for warfarin, phenylbutazone, azapropazone, etc., and site II for ibuprofen, flufenamic acid, diazepam, etc. The binding of digitoxin was found to be independent of sites I and II, which was defined as being at site III [33]. In the present study, the primary binding site of CoQ_{10}–HSA was confirmed at 298 K by competitive experiments using warfarin, ibuprofen, and digitoxin as site markers [34, 35]. The fluorescence spectra are shown in Fig. 6. As shown in Fig. 6a, with the addition of warfarin, the emission maximum of HSA has an obvious red shift, and the fluorescence intensity is remarkably lower than that of a solution without warfarin. With the addition of CoQ_{10}, the fluorescence intensity of HSA decreases gradually, along with an obvious blue shift. This indicates that the addition of warfarin had a significant influence on the binding

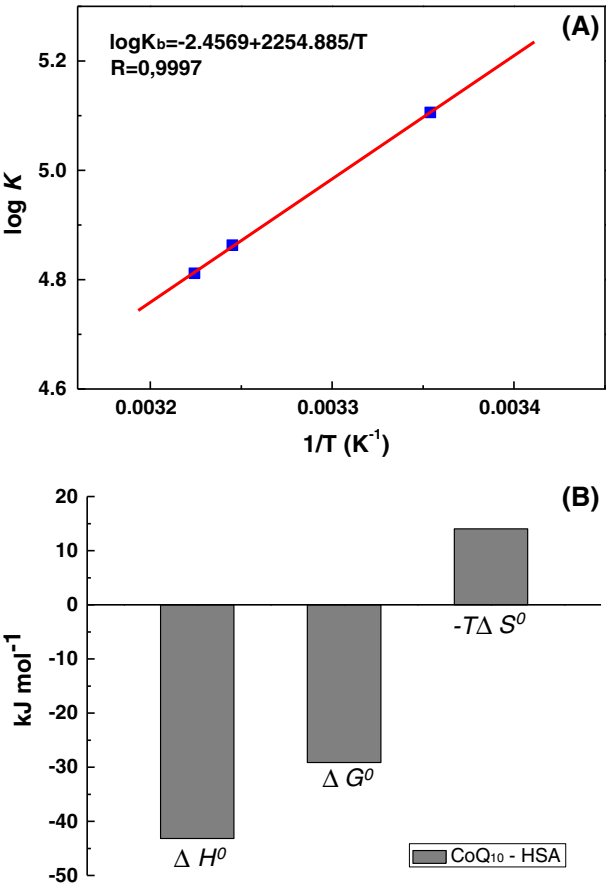

Fig. 5 **a** van't Hoff plot of HSA–CoQ_{10} system. **b** The *bar diagram* of thermodynamic parameters for the CoQ_{10}–HSA system

Table 3 Thermodynamic parameters of CoQ_{10}–HSA system

T (K)	ΔG^0 (kJ·mol^{-1})	ΔH^0 (kJ·mol^{-1})	ΔS^0 (J·mol^{-1}·K^{-1})	R
298	−29.15	−43.18	−47.05	0.9997
308	−28.68			
310	−28.59			

R correlation coefficient

of CoQ_{10} to HSA. From Fig. 6b it can be seen that, with the addition of ibuprofen, the fluorescence of HSA was almost the same as in the absence of ibuprofen. Figure 6c is similar to Fig. 6b. This indicates that the addition of ibuprofen or digitoxin has no significant influence on the binding of CoQ_{10}–HSA.

To confirm the binding site of CoQ_{10}–HSA, the binding constants of HSA–CoQ_{10} in the presence of site makers were estimated by Eq. 4. The values are calculated to be

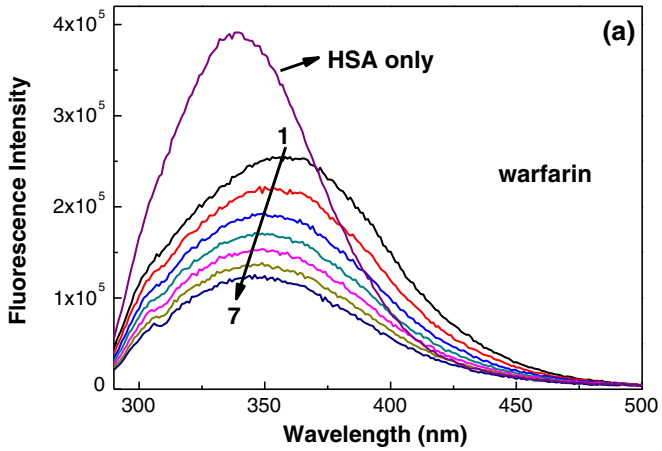
(a)
HSA only
1
7
warfarin
Fluorescence Intensity
Wavelength (nm)
4x10^5
3x10^5
2x10^5
1x10^5
0
300
350
400
450
500

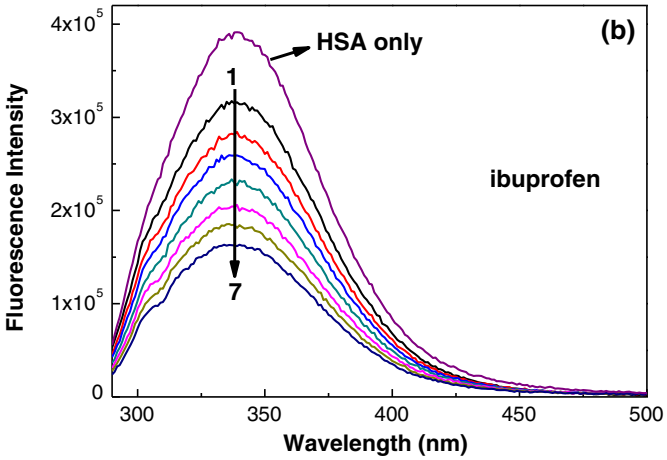
(b)
HSA only
1
7
ibuprofen
Fluorescence Intensity
Wavelength (nm)
4x10^5
3x10^5
2x10^5
1x10^5
0
300
350
400
450
500

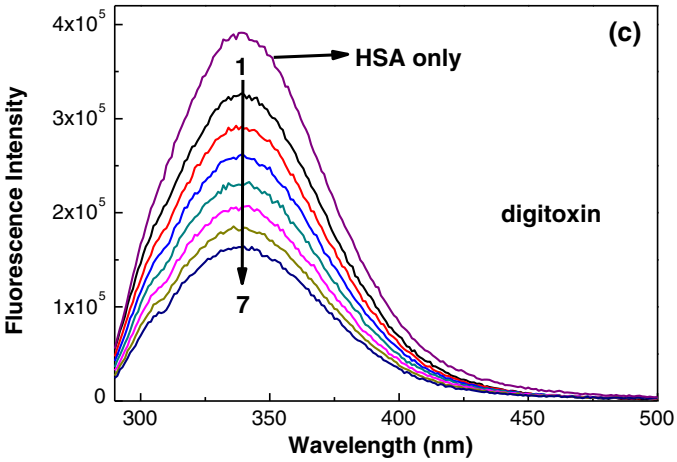
(c)
HSA only
1
7
digitoxin
Fluorescence Intensity
Wavelength (nm)
4x10^5
3x10^5
2x10^5
1x10^5
0
300
350
400
450
500

◀ **Fig. 6** Effect of site markers on the CoQ_{10}–HSA system (298 K, $\lambda_{ex} = 280$ nm). **a** Warfarin, **b** ibuprofen, and **c** digitoxin. The concentrations of HSA and all the markers were fixed at 5.0×10^{-6} mol·L^{-1}, and the concentrations of CoQ_{10} (*1–7*) were 0, 0.5, 1.0, 1.5, 2.0, 2.5 and 3.0×10^{-5} mol·L^{-1}

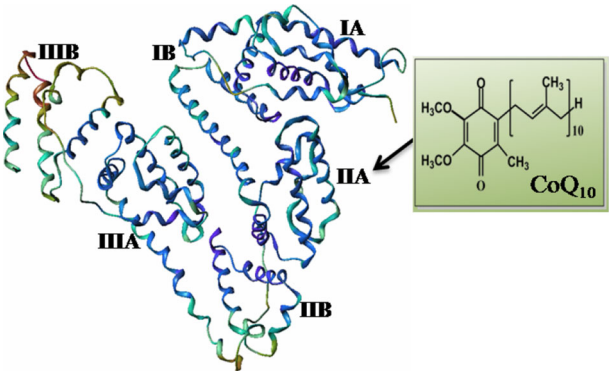

Fig. 7 3D structure of HSA and binding site of CoQ_{10} on HSA

0.466×10^5 L·mol^{-1} (warfarin), 0.990×10^5 L·mol^{-1} (ibuprofen), and 1.270×10^5 L·mol^{-1} (digitoxin). From Table 2, the binding constant of HSA–CoQ_{10} without site maker is 1.276×10^5 L·mol^{-1} at 298 K. It is obvious that the binding constant is significantly lower in the presence of warfarin, while there is a small influence on the binding parameter in the presence of ibuprofen (somewhat lower than that of HSA–CoQ_{10} without site maker), and almost no effect on the binding parameter in the presence of digitoxin. These differences in binding constants values in the absence and presence of site markers are significant enough to deduce the binding sites location as reported in the literature [23, 27]. These results suggest that the binding site of CoQ_{10} or warfarin is the same on HSA, so the binding site of CoQ_{10} is mainly located in site I (subdomain IIA) of HSA, as shown in Fig. 7.

3.6 Energy Transfer from HSA to CoQ_{10}

Fluorescence resonance energy transfer (FRET) is a non-radiative transfer of the excitation energy from a donor to an acceptor chromophore. It is mediated by a long-range interaction between the emission and absorption transition dipole moments of the donor and the acceptor, respectively [34]. FRET is also a good technique to evaluate the distance (in the nanometer range) between the donor (fluorophore) and acceptor in vitro and in vivo [36]. According to Förster's non-radiation energy transfer theory, energy transfer will happen at the following conditions: (a) the donor can produce fluorescence, (b) the donor's fluorescence emission spectrum and the acceptor's UV–vis absorbance spectrum overlap, and (c) the distance between the donor and the acceptor is no more than 8 nm.

The distance r between CoQ_{10} and HSA can be calculated by the following:

$$E = 1 - \frac{F}{F_0} = \frac{R_0^6}{R_0^6 + r^6}, \tag{7}$$

where E represents the efficiency of energy transfer between the donor (HSA) and the acceptor (CoQ_{10}), R_0 is the critical distance where the efficiency of energy transfer is 50 %

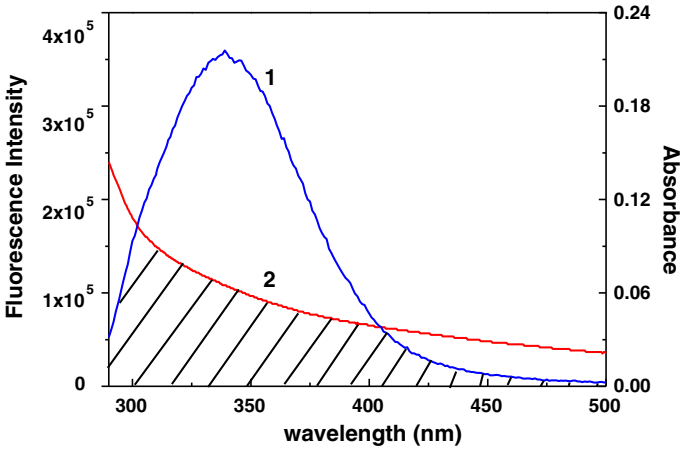

Fig. 8 Overlap between the fluorescence emission spectrum of HSA (*1*) and UV–vis absorption spectrum of CoQ_{10} (*2*), 298 K, pH = 7.40, and $\lambda_{ex} = 280$ nm

and can be calculated from donor emission and acceptor absorption spectra by using Förster's formula (Eq. 8):

$$R_0^6 = 8.79 \times 10^{-25} K^2 N^{-4} \Phi J, \tag{8}$$

where K^2 is the spatial orientation factor of the dipole and equals 2/3 for random orientation as in fluid solutions, N is the average refractive index of the medium, Φ is the fluorescence quantum yield of the donor, and J is the integral of the spectral overlap between the emission spectrum of the donor and the absorption spectrum of the acceptor, which is calculated by the following:

$$J = \frac{\sum F(\lambda)\varepsilon(\lambda)\lambda^4 \Delta\lambda}{\sum F(\lambda)\Delta\lambda}, \tag{9}$$

where $F(\lambda)$ is the fluorescence intensity of the donor when the wavelength is λ, and $\varepsilon(\lambda)$ is the molar absorption coefficient of the acceptor when the wavelength is λ. The overlap of the fluorescence emission spectrum of HSA with the absorption spectrum of CoQ_{10} is shown in Fig. 8. In the HSA–CoQ_{10} system, $K^2 = 2/3$, $N = 1.336$, and $\Phi = 0.15$ [36]. Hence, from Eqs. 7 to 9, we can calculate that $J = 1.784 \times 10^{-14}$ $cm^3 \cdot L \cdot mol^{-1}$, $R_0 = 2.81$ nm, $E = 0.0735$ and $r = 4.29$ nm. The values for (r) and (R_0) are within 8 nm, indicating that the energy transfer from HSA to CoQ_{10} can happen with high probability, and there is a static quenching interaction between HSA and CoQ_{10}.

3.7 Synchronous Fluorescence Spectroscopy

Synchronous fluorescence spectroscopy is frequently used to analyze the interaction between small molecules and proteins, since it can provide information about the molecular microenvironment in the vicinity of the fluorophore molecules [2]. It not only maintains the sensitivity associated with fluorescence, but also offers several advantages such as spectral simplification, spectral bandwidth reduction, and the avoidance of different perturbing effects. The shift in the maximum emission wavelength reflects the

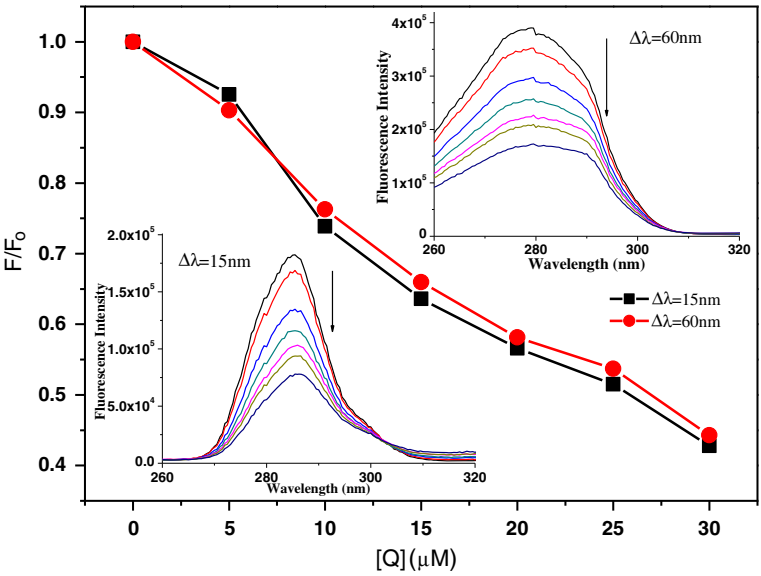

Fig. 9 The synchronous fluorescence spectra of HSA in the presence of CoQ_{10} at different $\Delta\lambda$ values (15 and 60 nm). The concentration of HSA was fixed at 5.0×10^{-6} mol·L^{-1} and the concentrations of CoQ_{10} (*1–7*) were 0, 0.5, 1.0, 1.5, 2.0, 2.5 and 3.0×10^{-5} mol·L^{-1}

change of polarity around a chromophore molecule. A blue shift of the maximum emission wavelength indicates a decreasing polarity of the surrounding environment, a higher hydrophobicity and a less loose structure of HSA, and vice versa [37]. The excitation and emission wavelength intervals ($\Delta\lambda$) were fixed at 15 and 60 nm, at which the spectrum shows conformational information of Tyr and Trp residues in HSA, respectively [38].

It is apparent from Fig. 9 that the emission of the Tyr and Trp residues show almost no shift at the investigated concentrations, indicating that the microenvironments and polarities around these residues underwent no large changes during the binding process. A similar fluorescence quenching profile was found for both Tyr and Trp residues upon addition of CoQ_{10}–HSA, which can be explained by that the Tyr and Trp residues of HSA may have equal accessibility to CoQ_{10}. Tyr residues such as Tyr-263, 319, 332, 334, 341, 353, and 370 are located in domain II of HSA with a hydrophobic environment, and Trp-214 is also located in this domain. The fluorescence changes suggest that the interaction between drug and HSA may occur in domain II, involving the Tyr and Trp residues [39]. Furthermore, the fluorescence intensity decreased regularly with the addition of CoQ_{10} in Fig. 9, which further demonstrates the occurrence of fluorescence quenching and the conformational changes in HSA.

3.8 Three-Dimensional Fluorescence Spectroscopy

To obtain further insight into the conformational changes involved in HSA with CoQ_{10} binding, three-dimensional fluorescence spectroscopy was performed on HSA both in the free form and in the complexed form. This is a fluorescence analytical technique developed in recent years that can comprehensively provide the fluorescence character of the sample, making investigation of the characteristic conformational changes of protein more

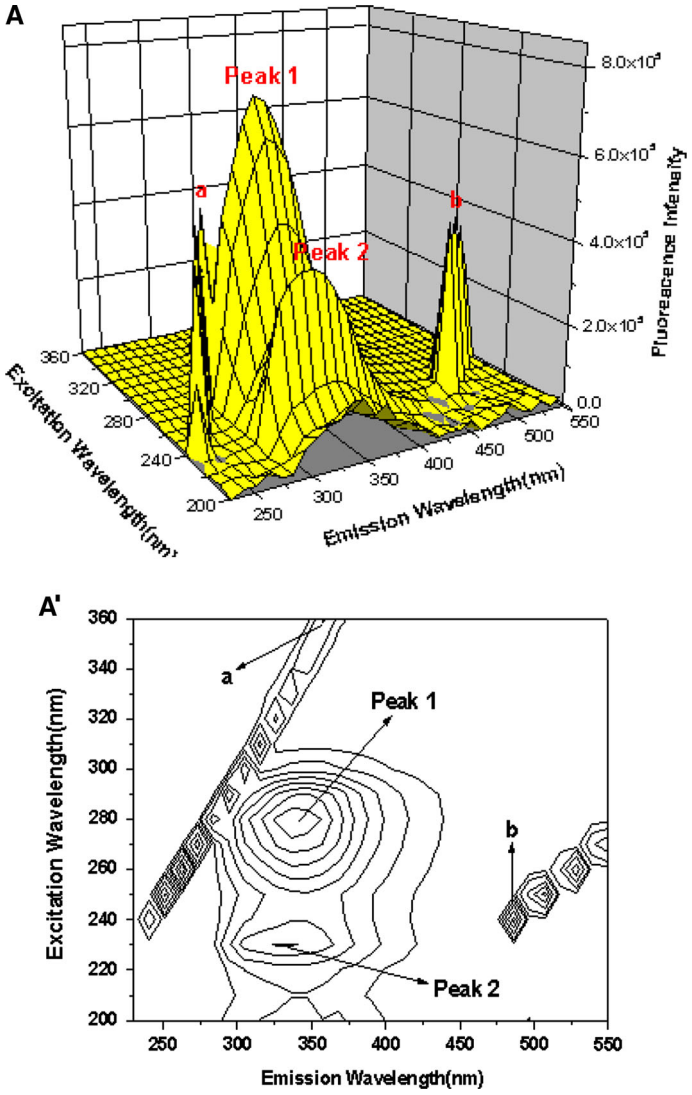

Fig. 10 The three-dimensional fluorescence spectra (**a**, **b**) and corresponding contour spectra (**a′**, **b′**) of the HSA and HSA–CoQ_{10} system. **a**, **a′** [HSA] = 5.0×10^{-6} mol·L^{-1}, [CoQ_{10}] = 0, **b**, **b′** [HSA] = 5.0×10^{-6} mol·L^{-1}, and [CoQ_{10}] = 10.0×10^{-6} mol·L^{-1}

convenient and credible. If there is a change at the excitation or emission wavelength of the fluorescence peak, emergence of a new peak, disappearance of some present peaks and so forth, then it would indicate that the conformation of the protein has undergone significant changes during the binding process [40]. The three-dimensional fluorescence spectroscopy and contour maps for HSA as well as for the HSA–CoQ_{10} system are shown in Fig. 10a, b and the corresponding characteristic parameters are collected in Table 4. As can be seen from Fig. 10a′, b′, peak a ($\lambda_{em} = \lambda_{ex}$), there is a Rayleigh scattering peak, and peak b ($\lambda_{em} = 2\lambda_{ex}$) represents the second-order scattering peak. It is important to note that the

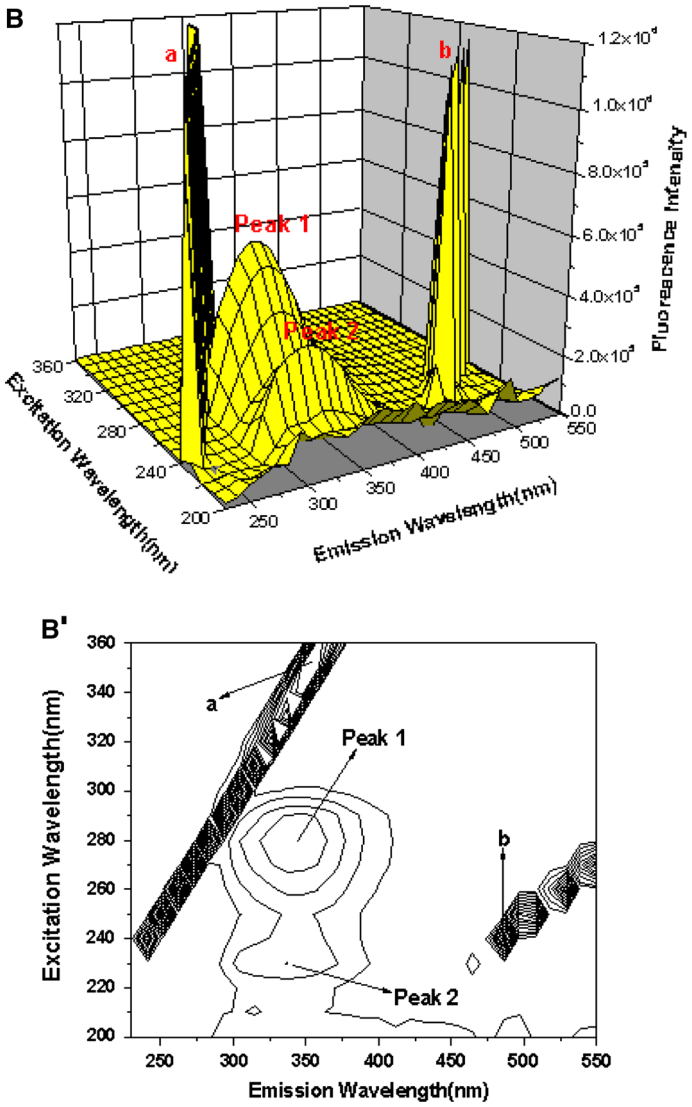

Fig. 10 continued

fluorescence intensities of both peaks increase with the addition of CoQ_{10}. The reason for this phenomenon is that formation of the HSA–CoQ_{10} complex increases the diameter of the macromolecule, and therefore leads to an enhanced scattering effect [37]. In addition to two scattering peaks, another two typical fluorescence peaks, 1 and 2 are found. Peak 1 ($\lambda_{ex} = 280.0$ nm, $\lambda_{em} = 336$ nm) mainly shows the spectral behavior of Trp and Tyr residues, because when HSA is excited at 280 nm, it primarily displays intrinsic fluorescence of the Trp and Tyr residues, and the fluorescence of the Phe residue can be negligible [39]. On the other hand, peak 2 ($\lambda_{ex} = 230.0$ nm, $\lambda_{em} = 333.5$ nm) is related to the fluorescence character of the polypeptide backbone structure of HSA caused by the $P \rightarrow P^*$ transition of structure C=O in the protein, and reflects changes in the secondary

Table 4 Three-dimensional fluorescence spectral characteristics of the HSA–CoQ_{10} system

Peaks	HSA			HSA–CoQ_{10}		
	Peak position $\lambda_{ex}/\lambda_{em}$ ($nm \cdot nm^{-1}$)	Stokes $\Delta\lambda$ (nm)	Intensity F	Peak position $\lambda_{ex}/\lambda_{em}$ ($nm \cdot nm^{-1}$)	Stokes $\Delta\lambda$ (nm)	Intensity F
Rayleigh scattering peak a	240/240 → 360/360	0	115.6 → 695.7	240/240 → 360/360	0	679.7 → 950.4
Fluorescence peak 1	280.0/336.0	56	609.5	280.0/345.5	65.5	465.4
Fluorescence peak 2	230.0/333.5	103.5	329.2	230.0/335.5	105.5	272.3

structure of HSA in the presence of CoQ_{10} [39]. The intensity of peak 2 decreased significantly after the addition of CoQ_{10}, which means that the structure of HSA was altered, and this coincided with the far-UV CD results below. Moreover, in the presence of CoQ_{10}, the fluorescence intensities of both peaks 1 and 2 decrease to different degrees along with a red shift (for 1 about 34 %, 4.5 nm, and for 2 about 18 %, 2 nm). The decrease of fluorescence intensities of the two peaks combined with the CD spectral results demonstrate that the addition of CoQ_{10}–HSA induced the small destabilization of the polypeptide chain of HSA, which results in a conformational change of HSA. From above analysis, it was found that the three-dimensional fluorescence maps of protein in the absence and presence of the drug are totally different, and confirm that the interaction between CoQ_{10} and HSA causes conformational and microenvironmental alterations in the protein molecule.

3.9 ANS Fluorescence Spectroscopy

The intrinsic fluorescence spectroscopy only indicates the structural change around aromatic amino acids groups, so more studies should be carried out to make a systematic investigation of the conformational change of HSA induced by the binding of CoQ_{10}. ANS is only slightly fluorescent in aqueous solutions, but if bound to the hydrophobic portions of proteins; its fluorescence intensity increases significantly, which makes ANS a useful surface hydrophobic probe of proteins due to its hydrophobicity and environmental sensitivity [41]. In order to see whether the binding of CoQ_{10} has any effect on the fluorescence spectroscopy of ANS bound to HSA, ANS fluorescence spectroscopy was carried out and the results are shown in Fig. 11. CoQ_{10} alone or CoQ_{10} incubated with ANS has negligible fluorescence intensities, suggesting there is no interaction between CoQ_{10} and ANS. In contrast, fluorescence intensity of the ANS–HSA system decreases with increasing concentrations of CoQ_{10}, but no significant shift in fluorescence emission peak was detected. These results indicate that CoQ_{10} can reduce the hydrophobic surface of HSA which causes the ANS fluorescence quenching.

3.10 FT-IR Spectroscopy

Additional evidence regarding the HSA–CoQ_{10} complex is from IR spectroscopy studies. FT-IR spectroscopy is a powerful and well established experimental technique for analysis

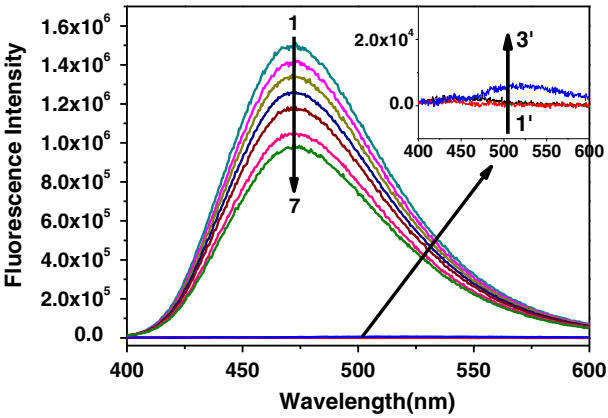

Fig. 11 Fluorescence quenching spectra of ANS bound HSA in the presence CoQ_{10}: [HSA] = 5.0×10^{-6} mol·L^{-1}, [ANS] = 15.0×10^{-6} mol·L^{-1} and the concentration of CoQ_{10} (*1–7*) is 0, 0.5, 1.0, 1.5, 2.0, 2.5 and 3.0×10^{-5} mol·L^{-1}, respectively. The inset shows the emission spectra of CoQ_{10} only (*1′*, 15.0×10^{-6} mol·L^{-1}), HSA only (*2′*, 5.0×10^{-6} mol·L^{-1}) and CoQ_{10} (*3′*, 15.0×10^{-6} mol·L^{-1}) incubated with ANS (15.0×10^{-6} mol·L^{-1}) under the same experimental conditions (λ_{ex} = 370 nm)

of the secondary structure of polypeptides and proteins [42]. It is convenient, non-destructive, requires less sample preparation, and can be used under a wide variety of conditions. When ligands are bound to a globular protein, the intramolecular forces responsible for maintaining the secondary and tertiary structures can be altered, resulting in a conformational change of the protein. For the protein, nine characteristic vibrational bands or group frequencies that arise from the amide groups of protein have been identified. Among them, amide I band (1,600–1,700 cm^{-1}, mainly the C=O stretch) and amide II band (1,500–1,600 cm^{-1}, C–N stretch coupled with N–H bending mode) have been widely accepted as the typical ones to be used, and they both have a relationship with the secondary structure of the protein [43]. However, the amide I band is found to be correlated closely with the change of protein secondary structure rather than amide II. The FT-IR spectra of free HSA and the difference spectra after binding with CoQ_{10} in phosphate buffer were recorded. It can be seen from Fig. 12 that the peak position of amide I band is shifted from 1,659.47 to 1,655.75 cm^{-1}, while that of amide II band moves from 1,547.60 to 1,543.87 cm^{-1}, along with the changes in the peak shape and peak intensity upon the addition of CoQ_{10} to HSA. These findings mean that the secondary structure of HSA was changed after binding with CoQ_{10}. The drug interacts with the C=O and C–N groups in protein that resulted in rearrangement of polypeptide carbonyl hydrogen bonding network [43].

3.11 CD Spectroscopy

To further ascertain the possible influence of CoQ_{10} on HSA, CD spectra measurements of HSA in the presence of CoQ_{10} were performed to provide additional evidence for the possible conformational changes of HSA. As shown in Fig. 13, two negative peaks at 208 and 220 nm were observed for HSA in the presence of CoQ_{10} with different concentrations. These peaks are known to correspond to π–π^* and n–π^* transfer of the α-helix peptide bond, respectively, which are typical spectral features indicating a protein rich α-helix structure [24, 44]. The fact that the CD spectra of HSA with and without CoQ_{10} are

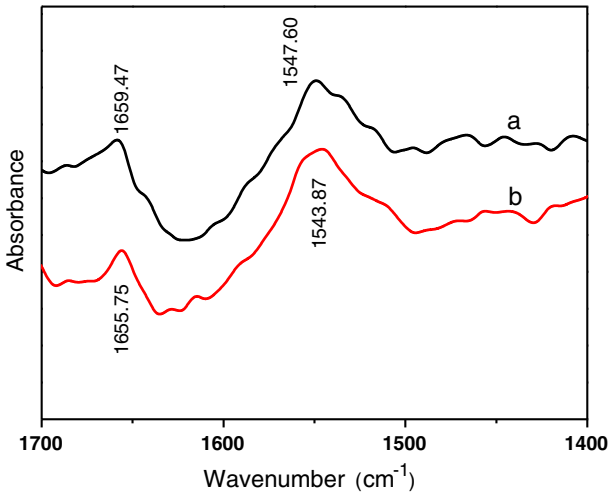

Fig. 12 (*a*) FT-IR spectra for free HSA and (*b*) difference spectra of HSA–CoQ_{10} complexes with the molar concentration ratio of HSA to drug of 1:4 in buffer solutions of pH = 7.4, [HSA] = 1.0×10^{-4} mol·L^{-1}, and [CoQ_{10}] = 4.0×10^{-4} mol·L^{-1}

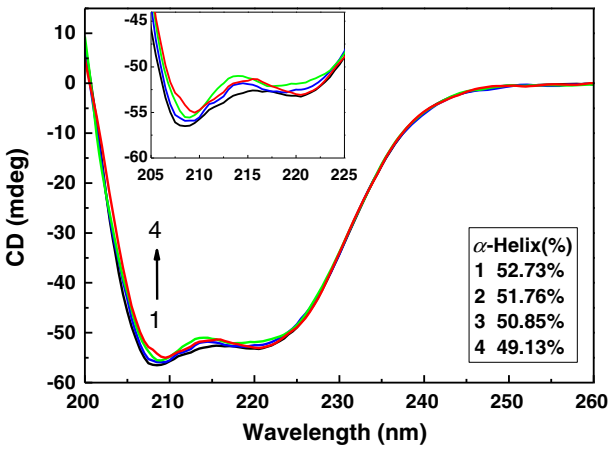

Fig. 13 CD spectra of the CoQ_{10}–HSA system. The concentration of HSA was fixed at 2.5×10^{-6} mol·L^{-1} and the concentrations of CoQ_{10} are 0 (*1*), 0.5×10^{-5} (*2*), 1.0×10^{-5} (*3*), and 1.5×10^{-5} mol·L^{-1} (*4*), respectively

similar in shape indicates that the structure of HSA is still predominantly α-helical even after binding to CoQ_{10}. The interaction of CoQ_{10} with HSA led to the decrease in both bands without any significant shifts, indicating some loss in the α-helix structure and the increase of disorder structure content of the protein. This might be the result of the formation of a complex between CoQ_{10} and HSA. Because the structure of HSA is predominant α-helical, in this paper we consider primarily the changes in the α-helical content of HSA. The content of α-helix in HSA can be calculated from the mean residue ellipticity (MRE) values at 208 nm by using the following Eqs. 10 and 11, as described by Greenfield and Fasman [45, 46]:

$$\mathrm{MRF} = \frac{\text{observed CD (m°)}}{C_p n l \times 10}, \tag{10}$$

$$\alpha\text{-helix } (\%) = \frac{[-\mathrm{MRE}_{208} - 4,000]}{[33,000 - 4,000]} \times 100, \tag{11}$$

where n is the number of amino acid residues in the protein, C_p is the concentration of protein (HSA) in mol·L^{-1}, l is the path length of cell in cm, MRE_{208} is the observed MRE value at 208 nm, 4,000 is the MRE value of the β-form and random coil conformation crossed at 208 nm, and 33,000 is the MRE value of a pure the α-helix at 208 nm.

The results (Fig. 13) show that the content of α-helix declined from 52.73 to 49.13 % as the concentration of CoQ_{10} increased from 0 to 1.5 × 10^{-5} mol·L^{-1}. This implies that the presence of CoQ_{10} can induce considerable changes in the secondary structure of HSA [47]. It also indicates that CoQ_{10} is bound with the amino acid residue of the main polypeptide chain of HSA, which diminished their hydrogen bonding networks [48]. The result is also in agreement with the results of the FT-IR experiments.

4 Conclusion

We used spectroscopic approaches to detect the binding of CoQ_{10}–HSA under physiological conditions. Analysis of the UV–vis spectra confirmed the binding of HSA with CoQ_{10} and the formation of a new complex. The results of the fluorescence spectra for the CoQ_{10}–HSA system demonstrate that the fluorescence quenching process is mainly controlled by a static quenching mechanism rather than a dynamic one. The number of binding sites (n) equals 1, so the molar ratio of CoQ_{10}–HSA is 1:1 when they are combined into a new complex. Thermodynamic parameters indicate that binding is a spontaneous process, and the main forces of binding between CoQ_{10} and HSA are hydrogen bonds and van der Waals forces. So, the binding is an enthalpy-driven process. The competitive experiments using different site markers indicate that subdomain IIA (site I) is the primary binding site of CoQ_{10}–HSA. Moreover, the secondary structure and micro-environmental of HSA are changed with the addition of CoQ_{10}, illustrated by the UV–vis absorption, synchronous fluorescence, three-dimensional fluorescence, ANS fluorescence, CD spectra, and FT-IR spectroscopy experiments. All of these results will be beneficial for investigating the pharmacokinetic and pharmacodynamic behavior of CoQ_{10} in pharmacology and clinical medicine. Furthermore, this study is also expected to provide important insight into the interactions of the physiologically important protein with other ligands.

Acknowledgments This work was supported by the Program for New Century Excellent Talents in Chinese University (NCET-08-0386), the 863 Program of China (2008AA10Z318, 2012AA06A303, 2013AA102204), the Natural Science Foundation of China (20976125, 31071509, 51173128) and Tianjin (10JCYBJC05100), the Ministry of Science and Technology of China (2012YQ090194), the Beiyang Young Scholar of Tianjin University (2012) and the Program of Introducing Talents of Discipline to Universities of China (Number B06006).

References

1. Cui, F.L., Yan, Y.H., Zhang, Q.Z., Qu, G.R., Du, J., Yao, X.J.: A study on the interaction between 5-methyluridine and human serum albumin using fluorescence quenching method and molecular modeling. J. Mol. Model. **16**, 255–262 (2010)
2. Suryawanshi, V.D., Anbhule, P.V., Gore, A.H., Patil, S.R., Kolekar, G.B.: Spectroscopic investigation on the interaction pyrimidine derivative, z-amino-6-hydroxy-4-(3,4-dimethoxyphenyl)-pyrimidine-5-carbonitrile with human serum albumin: mechanistic and conformational study. Ind. Eng. Chem. Res. **51**, 95–102 (2012)

3. Tousi, S.H., Saberi, M.R., Chamani, J.: Comparing the interaction of cyclophosphamide monohydrate to human serum albumin as opposed to holo-transferrin by spectroscopic and molecular modeling methods: evidence foe allocating the binding site. Protein Pept. Lett. **17**, 1524–1535 (2010)
4. Curry, S., Mandelkow, H., Brick, P., Franks, N.: Crystal structure of human serum albumin complexed with fatty acid reveals an asymmetric distribution of binding sites. Nat. Struct. Biol. **5**, 827–835 (1998)
5. Buttar, D., Colclough, N., Gerhardt, S., MacFaul, P.A., Phillips, S.D., Plowright, A., Whittamore, P., Tam, K., Maskos, K., Steinbacher, S., Steuber, H.: A combined spectroscopic and crystallographic approach to probing drug–human serum albumin interactions. Bioorg. Med. Chem. **18**, 7486–7496 (2010)
6. Pan, X.R., Qin, P.F., Liu, R.T., Wang, J.: Characterizing the interaction between tartrazine and two serum albumins by a hybrid spectroscopic approach. J. Agric. Food Chem. **59**, 6650–6656 (2011)
7. Darwish, S.M., Abu Sharkh, S.E., Abu Teir, M.M., Makharza, S.A., Abu-hadid, M.M.: Spectroscopic investigations of pentobarbital interaction with human serum albumin. J. Mol. Struct. **963**, 122–129 (2010)
8. Zhang, W.J., Xiong, X.J., Wang, F., Ge, Y.S., Liu, Y.: Studies of the interaction between ronidazole and human serum albumin by spectroscopic and molecular docking methods. J. Solution Chem. **42**, 1194–1206 (2013)
9. Frei, B., Kim, M.C., Ames, B.N.: Ubiquinol-10 is an effective lipid-soluble antioxidant at physiological concentrations. Proc. Natl. Acad. Sci. USA **87**, 4879–4883 (1990)
10. Itagaki, S., Ochiai, A., Kobayashi, M., Sugawara, M., Hiran, T., Iseki, K.: Interaction of coenzyme Q10 with the intestinal drug transporter *p*-glycoprotein. J. Agric. Food Chem. **56**, 6923–6927 (2008)
11. Crane, F.L.: Biochemical functions of coenzyme Q10. J. Am. Coll. Nutr. **20**, 591–598 (2001)
12. Shults, C.W., Oakes, D., Kieburtz, K., Beal, M.F., Haas, R., Plumb, S., Juncos, J.L., Nutt, J., Shoulson, I., Carter, J., Kompoliti, K., Perlmutter, J.S., Reich, S., Stern, M., Watts, R.L., Kurlan, R., Molho, E., Harrison, M., Lew, M.: Effects of coenzyme Q10 in early Parkinson disease: evidence of slowing of the functional decline. Arch. Neurol. **59**, 1541–1550 (2002)
13. Mancini, A., Festa, R., Raimondo, S., Pontecorvi, A., Littarru, G.P.: Hormonal influence on coenzyme Q10 levels in blood plasma. Int. J. Mol. Sci. **12**, 9216–9225 (2011)
14. Stocker, R., Bowry, V.W., Frei, B.: Ubiquinol-10 protects human low density lipoprotein more efficiently against lipid peroxidation than does α-tocopherol. Proc. Natl. Acad. Sci. USA **88**, 1646–1650 (1991)
15. Mizushina, Y., Takeuchi, T., Takakusagi, Y., Yonezawa, Y., Mizuno, T., Yanagi, K.-I., Imamoto, N., Sugawara, F., Sakaguchi, K., Yoshida, H., Fujita, M.: Coenzyme Q10 as a potent compound that inhibits Cdt1–geminin interaction. BBA Gen Subj **1780**, 203–213 (2008)
16. Qiu, L., Ding, H., Wang, W., Kong, Z., Li, X., Shi, Y., Zhong, W.: Coenzyme Q(10) production by immobilized *Sphingomonas* sp. ZUTE03 via a conversion–extraction coupled process in a three-phase fluidized bed reactor. Enzym Microb. Technol. **50**, 137–142 (2012)
17. Dimitrova, S., Pavlova, K., Lukanov, L., Zagorchev, P.: Synthesis of coenzyme Q10 and β-carotene by yeasts isolated from antarctic soil and lichen in response to ultraviolet and visible radiations. Appl. Biochem. Biotechnol. **162**, 795–804 (2010)
18. Lipshutz, B.H., Lower, A., Berl, V., Schein, K., Wetterich, F.: An improved synthesis of the "miracle nutrient" coenzyme Q10. Org. Lett. **7**, 4095–4097 (2005)
19. Soares, S., Mateus, N., Freitas, V.D.: Interaction of different polyphenols with bovine serum albumin (BSA) and human salivary α-amylase (HSA) by fluorescence quenching. J. Agric. Food Chem. **55**, 6726–6735 (2007)
20. Mahesha, H.G., Singh, S.A., Srinivasan, N., Rao, A.G.: A spectroscopic study of the interaction of isoflavones with human serum albumin. FEBS J. **273**, 451–467 (2006)
21. Chen, T., Cao, H., Zhu, S., Lu, Y., Shang, Y., Wang, M., Tang, Y., Zhu, L.: Investigation of the binding of Salvianolic acid B to human serum albumin and the effect of metal ions on the binding. Spectrochim. Acta A **81**, 645–652 (2011)
22. Kitamura, K., Omran, A.A., Takegami, S., Tanaka, R., Kitade, T.: ^{19}F NMR spectroscopic characterization of the interaction of niflumic acid with human serum albumin. Anal. Bioanal. Chem. **387**, 2843–2848 (2007)
23. Chi, Z., Liu, R.: Phenotypic characterization of the binding of tetracycline to human serum albumin. J. Agric. Food Chem. **12**, 203–209 (2011)
24. Lakowicz, J.R.: Principles of Fluorescence Spectroscopy, 3rd edn, pp. 277–285. Plenum Press, New York (2006)
25. Teng, Y., Liu, R.T., Li, C., Xia, Q., Zhang, P.J.: The interaction between 4-aminoantipyrine and bovine serum albumin: multiple spectroscopic and molecular docking investigations. J. Hazard. Mater. **190**, 574–581 (2011)

26. Wu, X., Liu, J., Huang, H., Xue, W., Yao, X., Jin, J.: Interaction studies of aristolochic acid I with human serum albumin and the binding site of aristolochic acid I in subdomain IIA. Int. J. Biol. Macromol. **49**, 343–350 (2011)
27. Hu, Y.J., Liu, Y., Xiao, X.H.: Investigation of the interaction between berberine and human serum albumin. Biomacromolecules **10**, 517–521 (2009)
28. Wang, W., Min, W., Chen, J., Wu, X., Hu, Z.: Binding study of diprophylline with lysozyme by spectroscopic methods. J. Lumin. **131**, 820–824 (2011)
29. Zhang, H., Huang, X., Zhang, M.: Spectral diagnostics of the interaction between pyridoxine hydrochloride and bovine serum albumin in vitro. Mol. Biol. Rep. **35**, 699–705 (2008)
30. Toneatto, J., Argüello, G.A.: New advances in the study on the interaction of $[Cr(phen)_2(dppz)]^{3+}$ complex with biological models; association to transporting proteins. J. Inorg. Biochem. **105**, 645–651 (2011)
31. Ding, F., Liu, W., Diao, J.X., Sun, Y.: Characterization of Alizarin Red S binding sites and structural changes on human serum albumin: a biophysical study. J. Hazard. Mater. **186**, 352–359 (2011)
32. Sudlow, G., Birkett, D.J., Wade, D.N.: The characterization of two specific drug binding sites on human serum albumin. Mol. Pharmacol. **11**, 824–832 (1975)
33. Brodersen, R., Sjödin, T., Sjöholm, I.: Independent binding of ligands to human serum albumin. J. Biol. Chem. **252**, 5067–5072 (1977)
34. Zhang, G., Wang, L., Pan, J.: Probing the binding of the flavonoid diosmetin to human serum albumin by multispectroscopic techniques. J. Agric. Food Chem. **60**, 2721–2729 (2012)
35. Zhang, G., Ma, Y.: Mechanistic and conformational studies on the interaction of food dye amaranth with human serum albumin by multispectroscopic methods. Food Chem. **136**, 442–449 (2013)
36. Lu, D., Zhao, X., Zhao, Y., Zhang, B., Geng, M., Liu, R.: Binding of Sudan II and Sudan IV to bovine serum albumin: comparison studies. Food Chem. Toxicol. **49**, 3158–3164 (2011)
37. Van de Hulst, H.C.: Light Scattering by Small Particles, pp. 383–446. Dover Publications, New York (1981)
38. Liu, W., Yang, T., Yao, C., Zuo, S., Kong, Y.: Spectroscopic studies on the interaction between troxerutin and bovine hemoglobin. J. Solution Chem. **42**, 1169–1182 (2013)
39. Wang, Y., Wang, X., Wang, J., Zhao, Y., He, W., Guo, Z.: Noncovalent interactions between a trinuclear monofunctional platinum complex and human serum albumin. Inorg. Chem. **50**, 12661–12668 (2011)
40. Cheng, Z., Zhang, L., Zhao, H., Liu, R., Xu, Q.: Spectroscopic investigation of the interactions of cryptotanshinone and icariin with two serum albumins. J. Solution Chem. **42**, 1238–1262 (2013)
41. Liu, M., Zhang, W., Qiu, L., Lin, X.: Synthesis of butyl–isobutyl-phthalate and its interaction with α-glucosidase in vitro. J. Biochem. **149**, 27–33 (2011)
42. Shen, H., Gu, Z., Jian, K., Qi, J.: In vitro study on the binding of gemcitabine to bovine serum albumin. J. Pharm. Biomed. Anal. **75**, 86–93 (2013)
43. Hemmateenejad, B., Shamsipur, M., Samari, F., Khayamian, T., Ebrahimi, M., Rezaei, Z.: Combined fluorescence spectroscopy and molecular modeling studies on the interaction between harmalol and human serum albumin. J. Pharm. Biomed. Anal. **67–68**, 201–208 (2012)
44. Liang, M., Liu, R., Qi, W., Su, R., Yu, Y., Wang, L., He, Z.: Interaction between lysozyme and procyanidin: multilevel structural nature and effect of carbohydrates. Food Chem. **138**, 1596–1603 (2012)
45. Chen, Y.H., Yang, J.T., Martinez, H.M.: Determination of the secondary structures of proteins by circular dichroism and optical rotatory dispersion. Biochemistry (US) **11**, 4120–4131 (1972)
46. Greenfield, N.J., Fasman, G.D.: Computed circular dichroism spectra for the evaluation of protein conformation. Biochemistry (US) **8**, 4108–4116 (1969)
47. Divsalar, A., Saboury, A.A., Haertlé, T., Sawyer, L., Mansouri-Torshizi, H., Barzegar, L.: Spectroscopic and calorimetric study of 2,2′-dibipyridin Cu(II) chloride binding to bovine β-lactoglobulin. J. Solution Chem. **43**, 705–715 (2013)
48. Zhang, G., Ma, Y., Wang, L., Zhang, Y., Zhou, J.: Multispectroscopic studies on the interaction of maltol, a food additive, with bovine serum albumin. Food Chem. **133**, 264–270 (2012)